Contents list available http://www.kinnaird.edu.pk/

Journal of Natural and Applied Sciences Pakistan

Journal homepage: http://jnasp.kinnaird.edu.pk/

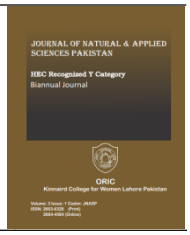

TEMPERATURE, TRANSMITTANCE AND SPECTRUM DEPENDENT SCATTERING IN ATMOSPHERE

Saddam Husain Dhobi [1,2,3,4]
Jeevan Jyoti Nakarmi[1,2,3]
Suresh Prasad Gupta[2,3]
Kishori Yadav[2,3]
Arun Kumar Shah[1,2]
Ram Lal Sah[5]
[1]Central Department of Physics, Tribhuvan University, Kirtipur, Kathmandu, Nepal
[2]Department of Physics, Patan Multiple Camus, Tribhuvan University, Lalitpur, Nepal
[3]Innovative Ghar Nepal, Lalitpur, Nepal
[4]Robotic Academy of Nepal, Lalitpur, Nepal
[5]Department of Physics, Padmakanya Multiple Campus, Tribhuvan University, Kathmandu, Nepal

Article Info

*Corresponding Author
Email: saddam@ran.edu.np

Abstract

Investigating the differential cross section (DCS) during the scattering of important atmospheric gases, including N_2, O_2, air, Ar, and CO_2, over a broad spectrum range from 0.2 μm to 100 μm, is the goal of this work. MATLAB was used to create a computational model that examined the nature of these interactions. Interesting information on the DCS values of the various gases is revealed by the study's observations. In particular, it was discovered that when the complete spectrum was taken into account, Ar DCS was higher than that of N_2, O_2, air, and CO_2. However, it was discovered that the DCS of N_2, O_2, and air was higher than that of Ar and CO_2 when taking transmittance and temperature into account at particular wavelengths. These comparisons were done at wavelengths of 0.3 μm, 0.6 μm, and 1.5 μm, respectively, respectively. These findings provide insight into the scattering characteristics of the investigated atmospheric gases. The higher DCS values for Ar across the whole spectrum range compared to N_2, O_2, air, and CO_2 point to a stronger interaction between Ar and incident radiation. However, the DCS values of N_2, O_2, and air take precedence over Ar and CO_2 when evaluating transmittance and temperature at particular wavelengths. The results of this study offer important new understandings of the scattering characteristics of the main atmospheric gases throughout a broad spectral range. The created computational model can aid in future research and improve our comprehension of atmospheric dynamics and radiative transfer phenomena.

Keywords
Differential Cross Section, Atmospheric Gases, Transmittance, Temperature, Spectral, Wavelength

1. Introduction

The primary sources of Rayleigh scattering are air molecules and other small particles. This happens when the wavelengths of the radiation interacting with the scattering particles have a significantly smaller diameter (less than one tenth) than those particles themselves. Selective or molecular scattering are additional names for Rayleigh scattering. This sort of visible electromagnetic radiation scattering is brought on by oxygen and nitrogen molecules, which predominate in the atmosphere (Shyama Prasad Mukherjee University, 2023). The scattering of electromagnetic waves by the atmosphere can be broadly separated into two types: selective scattering and nonselective scattering. Selective scattering is further subdivided into Rayleigh scattering and Mie scattering. Rayleigh scattering is the process through which air molecules such as oxygen, nitrogen, and others in the atmosphere scatter visible light (Liang and Wang, 2020). By using the Beer-Bouguer-Lambert law, the transmission of spectrum through a clear medium is correlated with its absorption coefficient,

$$t(x) = \frac{I}{I_0} = e^{-\beta_a x} \tag{1}$$

where t denotes transmission, β_a denotes the absorption coefficient, and x is the radiation's travel length. Equation (Sadrian *et al.,* 2023 & Bohren and Huffman, 1983) is used in order to compute the imaginary index of refraction (k).

$$k = \frac{\beta_a \lambda}{4\pi} \tag{2}$$

where λ the wavelength is used. For carbon dioxide concentrations of 100 and 400 ppm, respectively, absorption coefficients in the band centered at 4.3 μm subject to a specified optical path length of 104 m increase from 0.04 m^{-1} and 0.165 m^{-1} at the tropopause to 0.11 m^{-1} and 0.44 m^{-1} at the Earth's surface (Wei et al., 2018). Approximately 70% of the sun's rays that are directly overhead reach the Earth's surface through the atmosphere. However, the greenhouse gases absorb over 70% of the thermal radiation that is emitted from the Earth's surface (Wei et al., 2019). Equation (2) also provides $I(d) = I_0 \exp(-\beta_a . x)$. In this instance, the light's starting intensity is I_0, its intensity after traveling a distance of x is I(d), and β_a is defined as,

$$I(d) = I_0 \exp(-\beta_a . x) \tag{3}$$

$$\beta_a = \frac{1}{d} \log_{10} \left(\frac{I_0}{I} \right) \tag{4}$$

Hurter established the (optical) density in 1888 as the natural logarithm of the opacity, which, if reflectance is disregarded, is defined as 1, I/I_0 and equal to the fraction of light that is absorbed (Susanne and Popp, 2020). The fact that N_2 transmittance is all 1, regardless of height, throughout the troposphere, stratosphere, mesosphere, and thermosphere (Sun and Zheng, 2022) shows that the influence of N_2 on transmittance is constant.

Table 1: Adiabatic refractive index of few gases (Sneep, 2004),

Gases	**Refractive index**
O_2	1.40
N_2	
Air	
Ar	1.66
CO_2	1.31

For the study of temperature, transmittance, and spectrum-dependent scattering in the atmosphere, as well as for remote sensing, optical communication, astronomical observations, atmospheric physics, and remote sensing. It supports precise climate modeling, comprehension of atmospheric processes, improved interpretation of remote sensing data, optimization of optical communication systems, and improvement of astronomical measurements. Researchers learn more about climate change, air composition, and physical interactions by examining these events. They create models, algorithms, and corrective methods to enhance forecasts, data quality, and transmission effectiveness. This information aids in the development of numerous sectors, enhancing technologies, improving our understanding of the world, and increasing the validity of scientific observations.

2 Materials and methods

The above-described Rayleigh scattering holds true for a group of isotropic spherical particles. The molecules that make up air, primarily N_2 and O_2, are diatomic and, as a result, slightly anisotropic. Using a depolarization factor, it is possible to effectively account for molecular anisotropy by assuming molecular scattering to be a blend of real Rayleigh and isotropic scattering. The depolarization factor varies for various compounds and is slightly wavelength dependent. For air, depolarization equals 0.031 (McLinden, 2023). For the depolarization or correction factors of N_2 as a function of wavelength, Bates (1984) provided the following formula:

$$\delta(N_2) = 1.034 + 3.17 \times 10^{-4} \frac{1}{\lambda^2} \tag{5}$$

For O_2

$$\delta(O_2) = 1.096 + 1.385 \times 10^{-3} \frac{1}{\lambda^2} + 1.448 \times 10^{-4} \frac{1}{\lambda^4} \tag{6}$$

Additionally, δ(air) should be determined using equation (5) and (6), assuming that δ(Ar) = δ(He)= 1.00 (Wilmouth and Sayres, 2019), $\delta(CO_2)$= 1.15, and omitting the other components of air, according to Bates (1984). The "refractive index of air" experiment, which is frequently used in advanced undergraduate laboratories and optics courses. The average molecular polarizability of air, which is used to calculate the refractive index of air, is 2.133 ±0.032 × $10^{-29}$$m^3$ (95% CI), and the refractive index of air at atmospheric pressure is n = 1.0002651 (Madsen et al., 2011). Operationally, brown carbon is described as a carbonaceous material that absorbs

light and has an imaginary portion (k) of the complex refractive index that is wavelength dependent (Nakayama et al., 2013),

$$m = n - ki \tag{7}$$

More specifically, the scattering cross sections for H_2 range from $1.4 \times 10^{-38} m^2$ to $8.270 \times 10^{-33} m^2$ (Climate Policy Watcher Organization, 2023). Equation (9) (Abud, 2018) can be used to get the total Rayleigh scattering cross section by integrating over 4π steradians,

$$\sigma_R = \left(\frac{8}{3}\right)\left[\frac{\pi^2(n^2-1)^2}{N^2\lambda^4}\right] \tag{9}$$

Where N is the number of g/cm^3 gas molecules, n is the refractive index, and the scatter of the spectrum is determined analytically from equation (9), we get:

$$Q_{scat} = Q_{ext} = \left(\frac{8}{3}\right)\left(\frac{\pi d}{\lambda}\right)^4 \left[\frac{m^2-1}{m^2+1}\right]^2 \tag{10}$$

The scattering coefficient from equation (10) is found as, where Q_{sca} is the scattering efficiency, $\pi d/\lambda$ is known as the size parameter, m is the complex refractive index, d the diameter of the molecule, the wavelength, and $d = \frac{2\pi r}{\lambda}$

$$\sigma_m = \frac{32\pi^3(m-1)^2}{3\lambda^4} kT \frac{6+3\delta}{6-3\delta} \tag{11}$$

Form above equations (7), (2) and (4) we have

$$m = n - i\left\{\frac{1}{d}\log_{10}\left(\frac{I_0}{I}\right)\right\}\frac{\lambda}{4\pi} \tag{12}$$

Assuming transmittance 0 to 1, all wavelength (UV to Microwave: 0.2μ to 1 m) (Erath Observatory, 2023), and distance of troposphere 0 to 12 km (Global Climate Change, 2019). Now from (12) and (11) we have,

$$\sigma_m = \frac{32\pi^3\left(n - i\left\{\frac{1}{d}\log_{10}\left(\frac{I_0}{I}\right)\right\}\frac{\lambda}{4\pi} - 1\right)^2}{3\lambda^4} kT \frac{6+3\delta}{6-3\delta} \tag{13}$$

Transmittance of spectrum across the atmosphere ranges from 0 to 100% in different spectrum region 0.2μm (UV) to 100 μm (IR) (Earth Observatory, 1997). The transmittance in IR region ranges from 92% to 100% for CO_2 and O_2 (Kindel et al., 2015). The transmittance of spectrum through O_2 is ranges from 0 to 100% in visible region (Bertaux et al., 2014). Also, the transmittance of spectrum through atmosphere to space ranges from 0 to 100% in spectrum region 0 to 50μm (Giggenbach and Shrestha, 2022

3 Results and Discussion

3.1 DCS with wavelength of spectrum passing through troposphere

Figure 1 illustrates how the DCS decreases as the wavelength increases from UV to IR. Ar has a higher DCS than the molecules of O_2, N_2, air, and CO_2. Due to Ar's higher refractive index than other materials, the DCS of Ar is greater. Because of interactions between Ar and the spectrum, Ar's refractive index is larger than that of other materials. The velocity of the spectrum is inversely proportional to the speed or wavelength because $n = \frac{c}{v} = \frac{\lambda_c}{\lambda_m}$. As a result, the Ar medium's spectrum has a higher wavelength than molecules of O_2, N_2, air, and CO_2. Ar has a lesser interaction of its spectrum with electrons than other molecules due to its higher electron density. As a result, compared to other molecules, Ar has a stronger magnetic field that repels light. This repulsion results in a higher DCS, and figure 1 illustrates that the DCS of CO_2 is lower than that of O_2, N_2, air, and CO_2 molecules because its electron density is lower.

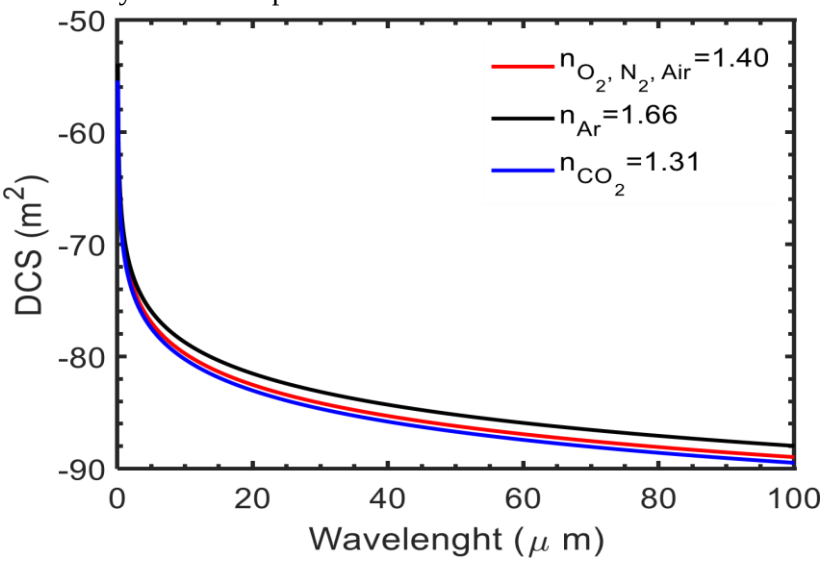

Figure 1: DCS with wavelength of atmospheric major gases present in troposphere

3.2 DCS with transmittance of spectrum passing through troposphere

Figure 2 illustrates the DCS of O_2, N_2, air, Ar, and CO_2 molecules with spectrum transmittance in the UV, visible (Vis), and infrared (IR) regions. According to the results, O_2, N_2, and air have consistent and higher DCS values than do Ar and CO_2 molecules. The DCS of O_2, N_2, and air was also measured at a wavelength of 0.3 μm in the UV region, the DCS of Ar at 0.6 μm in the visible spectrum, and the DCS of CO2 at 1.5 μm in the IR region. As opposed to Ar and CO_2, O_2, N_2, and air have constant and higher DCS values, which suggests that the former molecules are more prone to scatter or interact with incident radiation. Numerous reasons, including chemical structure, electrical transitions, or vibrational modes, could be at blame for this. O_2, N_2, and air have strong interactions with shorter-wavelength radiation, according to the discovery that the DCS of these molecules was observed in the UV region (0.3μm). This might be explained by the molecules' internal electronic transitions, which are frequently more apparent in the UV region. The DCS measurements for Ar in the visible spectrum (0.6 μm) and CO_2 in the IR spectrum (1.5μm) show that these chemicals interact more

strongly with longer-wavelength radiation, on the other hand. It is possible that the molecular characteristics and energy levels involved in scattering or absorbing incident light vary as a result of this variance in interaction wavelengths. due to the fact that the measurement is in the lower energy UV, Vis, and IR area. Figure 1's DCS measurement demonstrates that while DCS are quite dispersed and extremely variable at higher wavelengths, they are very close at short wavelengths.

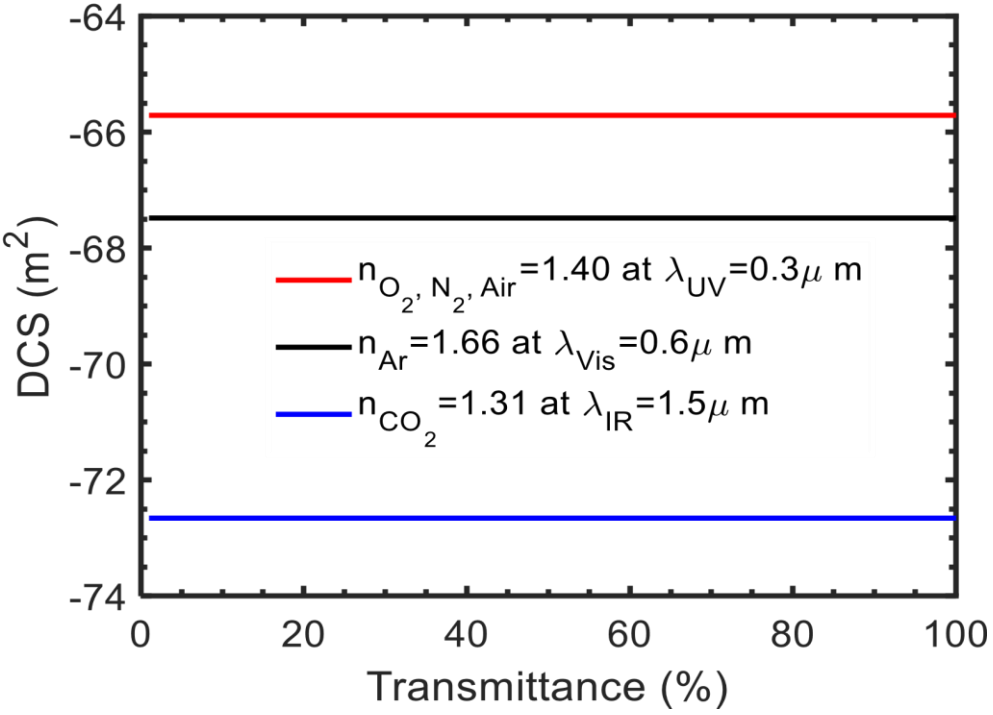

Figure 2: DCS with transmittance through atmospheric major gases present in troposphere

3.3 DCS with temperature when spectrum passing through troposphere

Figure 3 shows the DCS (differential cross section) of the main atmospheric constituents O_2, N_2, air, Ar, and CO_2 in relation to tropospheric temperature. The results show that the DCS values for O_2, N_2, and air at wavelengths of 0.3 μm, 0.6 μm, and 1.5 μm, respectively, are higher than those of Ar and CO_2. This mismatch can be ascribed to the spectral region's stronger interactions with air, N_2, and O_2 molecules than with Ar and CO_2 molecules. Additionally, the sizes of O_2, N_2, and air are equivalent at the wavelengths under consideration, however at the temperature under consideration, the sizes of Ar and CO_2 are drastically different. The observations in Figure 3 provide crucial new understandings of the key atmospheric elements' interactions with DCS and tropospheric temperature. When compared to Ar and CO_2, the higher DCS values for O_2, N_2, and air at particular wavelengths indicate that these molecules interact with incident radiation more forcefully. This can be explained by elements that affect how light is scattered or absorbed, such as molecule structure, electrical transitions, or vibrational modes. The observed DCS changes also depend on the sizes of the molecules. O_2, N_2, and air all exhibit equivalent sizes at the wavelengths and temperature under consideration, which would explain why their DCS values are similar. Contrasting DCS values are produced by the size differences between Ar and CO_2, on the other hand. The impact of temperature on the DCS is

another important consideration. The molecules of O_2, N_2, air, Ar, and CO_2 absorb thermal energy when the temperature rises, stretching their bonds and growing the molecules' and atoms' overall sizes. Higher DCS values may result from this size increase's influence on the molecules' scattering or absorption behavior. Therefore, the electron density of the atoms and molecules (described in Figure 1) is dominant overridden by the effects of temperature. As a result, as the temperature rises, the DCS values for O_2, N_2, and air dominate over those for Ar and CO_2. Overall, the findings demonstrate the intricate interactions between temperature and the DCS of atmospheric components. DCS values can vary for a variety of reasons, including chemical interactions, molecule sizes, and the impact of temperature-induced structural changes. To completely comprehend these linkages and their significance for atmospheric processes and radiative transfer, more investigation and analysis are required.

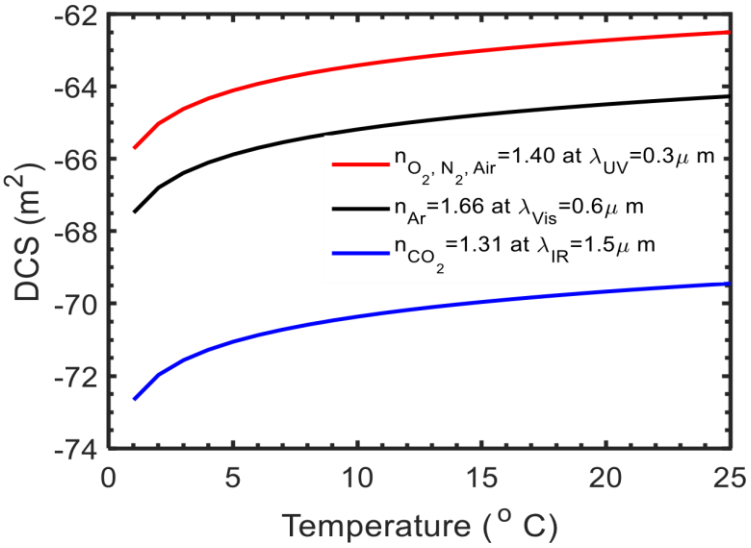

Figure 3: DCS with temperature of atmospheric major gases present in troposphere

4. Conclusion

In conclusion, several significant conclusions are shown by the DCS analysis of the main atmospheric gases, including N_2, O_2, air, Ar, and CO_2. From the UV to the IR area, the DCS values show a decrease with increasing wavelength. In addition, it is discovered that Ar has a greater DCS than N_2, O_2, air, and CO_2 molecules. Moving on to the investigation of DCS with transmittance of spectrum travelling through the troposphere, it has been observed that O_2, N_2, and air have greater DCS values than Ar and CO_2 and that these values are constant. The DCS data show that these compounds interact differently with various wavelength ranges in the UV, Vis, and IR areas. In terms of tropospheric temperature, the DCS values for O_2, N_2, and air are higher than those for Ar and CO_2 at particular wavelengths. The study emphasizes the intricate connections between chemical characteristics, wavelength, temperature, and the DCS of atmospheric components. To fully comprehend these interactions and their effects on radiative transport and atmospheric processes, more study is required.

Acknoledgment

Authors would like to thanks all members of innovative ghar Nepal for providing reserch space and peaceful environment during this reserch work.

References

Abud, M. M. (2018). Measure of Backscatter for small particles of atmosphere by lasers. Journal of Physics: Conference Series, 1003, 012079. doi: 10.1088/1742-6596/1003/1/012079

Bertaux, J. L., Lallement, R., Ferron, S., Boonne, C., & Bodichon, R. (2014). TAPAS, a webbased service of atmospheric transmission computation for astronomy?. Astronomy and Astrophysics, 564, A46. doi: 10.1051/0004-6361/201322383.

Bohren, C. F., & Huffman, D. R. (1983). Absorption and Scattering of Light by Small Particles. Wiley-Interscience.

Climate Policy Watcher Organization. (2023). Scattering by molecules Rayleigh scattering. Retrieved from https://www.climate-policy-watcher.org/surface-temperature/scatteringby-molecules-rayleigh-scattering.html

Erath Observatory. (2023). Remote Sensing: Absorption Bands and Atmospheric Windows. Retrieved from https://earthobservatory.nasa.gov/features/RemoteSensing/remote_04.php

Earth Observatory. (1997). Remote Sensing: Absorption Bands and Atmospheric Windows. NASA. Retrieved from https://earthobservatory.nasa.gov/features/RemoteSensing/remote_04.php

Giggenbach, D., & Shrestha, A. (2022). Atmospheric absorption and scattering impact on optical satellite-ground links. International Journal of Satellite Communications and Networking, 40, 157-176. https://doi.org/10.1002/sat.1426.

Global Climate Change. (2019). Earth's Atmosphere: A Multi-layered Cake. Retrieved from https://climate.nasa.gov/news/2919/earths-atmosphere-a-multi-layered-cake/#:~:text=From%20lowest%20to%20highest%2C%20the,%2C%20mesosphere%2C%20thermosphere%20and%20exosphere

Kindel, B. C., Pilewskie, P., Schmidt, K. S., Thornberry, T., Rollins, A., & Bui, T. (2015). Uppertroposphere and lower-stratosphere water vapor retrievals from the 1400 and 1900 nm water vapor bands. Atmospheric Measurement Techniques, 8, 1147-1156. doi: 10.5194/amt-8-1147-2015.

Liang, S., & Wang, J. (Editor). (2020). Chapter 4 - Atmospheric correction of optical imagery. In Advanced Remote Sensing (Second Edition) (pp. 131-156). Academic Press. https://doi.org/10.1016/B978-0-12-815826-5.00004-0

McLinden, C. (2023). Depolarization by Air. Retrieved from https://www.ess.uci.edu/~cmclinden/link/xx/node21.html.

Madsen, M. J., Brown, D. R., Krutz, S. R., & Milliman, M. J. (2011). Measuring the Molecular Polarizability of Air. American Journal of Physics, 79(4). http://dx.doi.org/10.1119/1.3533354

Nakayama, T., Sato, K., Matsumi, Y., Imamura, T., Yamazaki, A., & Uchiyama, A. (2013). Wavelength and NOx dependent complex refractive index of SOAs generated from the photooxidation of toluene. Atmospheric Chemistry and Physics, 13, 531-545. http://www.atmos-chem-phys.net/13/531/2013/

Shyama Prasad Mukherjee University (2023). Module – 1 Lecture Notes – 3: Energy Interactions in the Atmosphere [Lecture notes]. Dr. Shyama Prasad Mukherjee University, Ranchi. Retrieved from https://www.dspmuranchi.ac.in/pdf/Blog/04_ENERGY%20INTERACTIONS%20IN%2 0THE%20ATMOSPHERE.pdf

Sadrian, M. R., Calvin, W. M., Perrin, A. E., Engelbrecht, J. P., & Moosmüller, H. (2023). Variations in Infrared Complex Refractive Index Spectra of Surface Soils from Global Dust Entrainment Regions. Atmosphere, 14, 675. https://doi.org/10.3390/atmos14040675

Susanne, T. M., & Popp, P. J. (2020). The Bouguer-Beer-Lambert Law: Shining Light on the Obscure. ChemPhysChem, 21(18), 1-19. doi: 10.1002/cphc.202000464.

Sun, D., & Zheng, H. (2022). Simulation Study of Infrared Transmittance Under Different Atmospheric Conditions. Journal of Physics: Conference Series, 2356, 012045. doi: 10.1088/1742-6596/2356/1/012045.

Sneep, M. (2004). The atmosphere in the laboratory: cavity ring-down measurements on scattering and absorption [Doctoral dissertation, Vrije Universiteit]. Retrieved from http://www.nat.vu.nl/~wimu/PhD-Theses/Maarten-Sneep-Thesis.pdf.

Wei, P. S., Hsieh, Y. C., Chiu, H. H., Yen, D. L., Lee, C., Tsai, Y. C., & Ting, T. C. (2018). Absorption coefficient of carbon dioxide across atmospheric troposphere layer. Heliyon, 4(10), e00785. doi: 10.1016/j.heliyon.2018.e00785

Wei, P. S., Chiu, H. H., Hsieh, Y. C., Yen, D. L., Lee, C., Tsai, Y. C., & Ting, T. C. (2019). Absorption coefficient of water vapor across atmospheric troposphere layer. Heliyon, 5(1), e01145. doi: 10.1016/j.heliyon.2019.e01145.

Wilmouth, D. M., & Sayres, D. S. (2019). Rayleigh scattering cross sections of argon, carbon dioxide, sulfur hexafluoride, and methane in the UV-A region using Broadband Cavity Enhanced Spectroscopy. Journal of Quantitative Spectroscopy and Radiative Transfer, 234, 32-39. doi: 10.1016/j.jqsrt.2019.05.031.